Optimization of Nonlinear Optical Properties by Substituent Position, Geometry and Symmetry of the Molecule: An ab Initio Study

Daly Davis and K. Sreekumar

Department of Applied Chemistry, Cochin University of Science and Technology, Cochin 682 022, India

Y. Sajeev and Sourav Pal*

Theory group, Physical Chemistry Division, National Chemical Laboratory, Pune 411 008, India

Received: March 15, 2005; In Final Form: May 26, 2005

Static polarizability and first- and second-order hyperpolarizability tensors are computed at the correlated level for a series of *para*-nitroaniline derivatives. The importance of including electron correlation effects in the determination of equilibrium structure and the molecular properties is investigated. A qualitative description of the substitution effects, planarity, and symmetric effect of the molecule on the molecular susceptibility is discussed.

I. Introduction

Nonlinear optics is playing a major role in the light-intensity-dependent transmission properties of materials and in the technology of photonics. The strong oscillating electric field of laser creates a polarization response that is nonlinear in character and that can act as a source of new optical fields with altered properties.[1] The nonlinear optical (NLO) susceptibilities of a material provide a quantitative measure of the ability of a bulk material to alter the optical properties and are the parameters that researchers in NLO materials seek to optimize. One can define microscopic nonlinear coefficients (molecular hyperpolarizabilities) that are the molecular equivalents of bulk nonlinear optical susceptibilities. In fact, the bulk susceptibilities can be readily related to the susceptibilities of the constituent molecules. Hyperpolarizabilities may be deduced experimentally from direct observations of harmonic generations[2] and from the measurements of the Kerr effect.[3] However, the experiments are difficult, and the range of uncertainty is often large. Since the hyperpolarizability is a property of a single atom or a molecule, it may be predicted from quantum mechanical calculations.[4]

The general theory underlying the calculation of nonlinear electric properties is already well-developed.[5] However, most research in this area is still being focused on the study of relatively small molecules for which the corresponding calculations can be made both accurate and conclusive.[6−9] An important development in nonlinear optical material occurred in 1970, when Davydov et al.[10] reported a strong second harmonic generation (SHG) in organic materials having electron donor and acceptor groups connected with a benzene ring. The optically induced polarization in these dyes generates the largest nonresonant (nonabsorptive) optical nonlinearities over a wide frequency range. Certain dye chromophoric systems restrict their applications to NLO devices, although they have parallel potentials in applications associated with light absorption, light emission, photoelectrical activity, and chemical and photochemical activities.[11] Since the field of nonlinear optics is uniquely concerned with the molecular design of fundamental dyes in which NLO response is governed largely by the chromophores involving interactions with light, the optical nonlinearity is primarily derived from molecular structure. The primary step in optimizing optical nonlinearities in this class of materials is at the molecular structural level, which then requires a detailed understanding of the relationship between molecular electronic structure and nonlinear polarization that can be induced in the molecule.[12] An understanding of the structure−property relations for the NLO responses provides guidelines for the design of novel molecular and polymeric NLO materials. Quantum chemistry can help to rationalize the experimental results and rank the existing molecular structures according to their linear and nonlinear susceptibilities prior to experiment and thus to propose new promising compounds to chemists. At the molecular level, the NLO properties are determined by first and second hyperpolarizabilities. One of the main issues in the calculation of nonlinear electric properties is the role of the electron correlation effects,[13] which need to be carefully studied.

Nonlinear optical properties of a variety of linear push−pull phenylenes have been extensively studied over the last two decades.[14,15] It was known that the NLO properties of these molecules are sensitive to many factors such as the conjugation length, donor and acceptor substitutions, and symmetric effects.[16] The *para*-nitroaniline (PNA) derivatives are the favorite test systems for investigation of different aspects of the accuracy and computational methodology used in calculations of nonlinear electric properties.[6,8] Frequency-dependent polarizabilities and hyperpolarizabilities of PNA were calculated by Ågren et al. using multiconfiguration self-consistent field (SCF)-based response approach.[17] The solvent effect on the hyperpolarizability and their frequency dispersion has been studied by Mikkelsen et al.[18] Champagne et al. applied a density functional theory (DFT)-based approach for the calculation of nonlinear optical properties of PNA.[19] With a double harmonic oscillator approximation, the vibrational contributions to the polarizability and first and second hyperpolarizability tensors of PNA for different optical processes by adopting the infinite frequency

* Electronic mail: pal@ems.ncl.res.in.

10.1021/jp051355d CCC: $30.25
Published on Web 06/30/2005

or enhanced approximation have been calculated by Champagne.[20] The first-order zero-point vibrational averaging correction for second harmonic generation in PNA have been determined analytically at the time-dependent Hartree−Fock level of approximation.[21]

Both the structure−property relationships and the effect of electron correlation on NLO properties will be considered in this paper and exemplified by the calculations of electric properties of PNA derivatives. The paper is organized as follows: In section II, we briefly introduce a minimal number of concepts about optical nonlinearities and the quantum chemical methods applied for the calculations. Section III discusses the computational details used in our calculations. Section IV contains the results of a second-order Møller−Plesset (MP) perturbation calculation of the electric field responses of PNA and its derivatives. Conclusions are given in Section IV.

II. General Theoretical Background

The problem of propagation of light in a medium is completely specified when the relations (constitutive relations) between the polarization and magnetization and the optical field are given. The electric polarization of the medium can be expanded according to the power of the applied field, F

$$P_I = \sum_J \chi_{IJ}^{(1)} F_j + \frac{1}{2}\sum_{JK} \chi_{IJK}^{(2)} F_J F_K + \frac{1}{6}\sum_{JKL} \chi_{IJKL}^{(3)} F_J F_K F_L + \ldots \quad (1)$$

where the indices I, J, K, and L run over the macroscopic axes of the material, and χ_{ijk}^{n} is the nth-order electric susceptibility, which is an $n + 1$ rank tensor. The first-order susceptibility describes the linear optical effects, while the remaining terms describe the nth-order nonlinear optical effects. For an isolated compound in an applied electric field, the polarizability (α) and hyperpolarizabilities (β, γ, ...) are the free-compound properties which can be calculated by quantum chemistry methods. The molecular response that relates the dipole moment, μ, upon interaction with a field, F, as

$$\mu_i(F) = \mu_i + \sum_j \alpha_{ij} F_j + \frac{1}{2}\sum_{jk} \beta_{ijk} F_j F_k + \frac{1}{6}\sum_{jkl} \gamma_{ijkl} F_j F_k F_l \ldots \quad (2)$$

where i, j, k, and l label the x, y, and z components with respect to the reference frame in which the molecular system is described. In this contribution, only the time-independent (static or frequency-independent) molecular responses will be considered. They can be calculated by taking the derivatives of the induced dipole moment of the system

$$\alpha_{ij} = \left.\frac{\delta \mu_i}{\delta F_j}\right|_{F=0} \quad (3)$$

$$\beta_{ijk} = \left.\frac{\delta^2 \mu_i}{\delta F_j\, \delta F_k}\right|_{F=0} \quad (4)$$

$$\gamma_{ijkl} = \left.\frac{\delta^3 \mu_i}{\delta F_j\, \delta F_k\, \delta F_l}\right|_{F=0} \quad (5)$$

An analogous formulation for α, β, and γ coefficients can be obtained by examining the molecular energy expansion

$$E(F) = E^0 - \sum_i \mu_i F_i - \sum_{ij} \alpha_{ij} F_i F_j - \frac{1}{2}\sum_{ijk} \beta_{ijk} F_i F_j F_k - \frac{1}{6}\sum_{ijkl} \gamma_{ijkl} F_i F_j F_k F_l \ldots \quad (6)$$

rather than the dipole expansion, with respect to the field.

There are two basic methodologies that can be used in an electronic structure method to compute the polarizabilities.[16] The first method, known as the sum-over-state (SOS) method,[22,23] is based on a perturbative scheme, in which the calculations are carried out on the free (independent of field) molecules and the response involves the coupling of excited states. The second method, the so-called finite-field (FF) approach,[24,25] basically relies on direct numerical differentiation techniques. The relevant system is the molecule in the presence of an external static electric field. The corresponding Hamiltonian

$$\hat{H}(F) = \hat{H}^0 - \sum_\sigma F \cdot r_\sigma \quad (7)$$

is diagonalized to calculate the ground-state energy (eq 2) (or dipole moment (eq 6)) at different F values, and (hyper)-polarizabilities are calculated as numerical derivatives of the energy (or dipole moment) with respect to the electric field (as given in eqs 3−5). In this formulation, the molecular Hamiltonian explicitly includes a term $\sum_\sigma F \cdot r_\sigma$ describing the interaction between the external uniform static field and the system, where σ labels the electron. In practice, the derivatives could be computed using numerical differentiation strategies. The main advantage of FF over SOS is that it requires only the ground-state energy (or dipole moment), whereas the SOS requires all the eigenstates and transition dipole moments. Calculation of dynamical properties have been implemented for most of the standard quantum chemical approaches using a time-dependent response technique, such as time-dependent Hartree−Fock (TDHF),[26] time-dependent Møller−Plesset (TDMP),[27] and the equation of motion coupled cluster (EOMCC)[28] methods.

The standard ab initio methods solve the Schrödinger equation in a direct way. The simplest approximation is the Hartree−Fock approximation, where the wave function is a Slater determinant composed of molecular orbitals. The finite-field self-consistent field (SCF−FF) was originally proposed by Cohen and Roothaan[24] and is equivalent to an analytic coupled Hartree−Fock scheme, standing out for its simplicity. The FF version of the Hartree−Fock method provides acceptable and useful estimates of the polarizability components α_{ij}. This is because the FF approach takes into account directly, and in a self-consistent way, the orbital relaxations in the presence of the perturbing external electric field. The components of the (hyper)polarizability tensors are obtained from derivatives of the field-dependent dipole moment with respect to the external electric field in the limit of zero fields. In practice, the components α_{ij} are evaluated numerically by using the following approximation for differentiating the dipole moment components with respect to the field:

$$\alpha_i = \left(\frac{\partial \langle \mu_i \rangle}{\partial F_i}\right)_{F=0} = \frac{1}{2F_i}[\mu_i(F_i) - \mu_i(-F_i)] \quad (8)$$

Improvements in the HF method are achieved using methods such as configuration interaction (CI), many-body perturbation theory (MBPT), and coupled cluster theory.

In principle, the strategies for the ab initio methods mentioned above are rigorous. All these methods tend to obtain better and

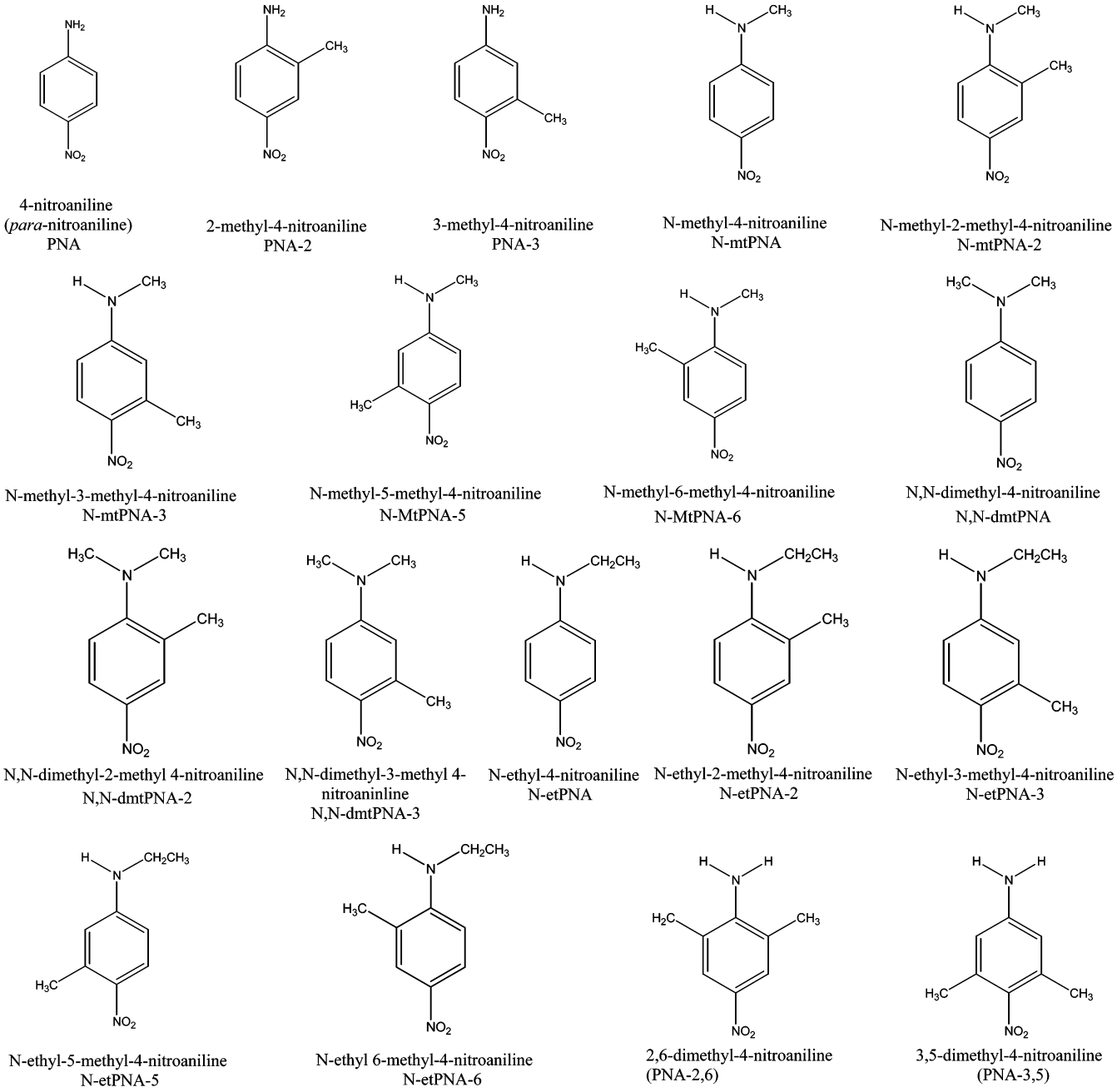

Figure 1.

better solution to the Schrödinger equation, but simultaneously demand larger and larger basis sets in order to take advantage of the higher degree of treatment of the correlation energies. A simple class of correlated ab initio theories use Rayleigh−Schrödinger perturbation expansion including correlation at a different order of perturbation in a size-extensive manner and are known as different MP(n) or MBPT(n) methods. The simplest MP2 itself captures the dominant correlation effects, without being computationally too demanding. It appears, on the basis of a number of studies on small molecules, that the MP2 treatment is adequate for describing at least 90% of the effects of electron correlation on static hyperpolarizabilities.

III. Computational Details

The molecules considered in this work are shown in Figure 1. The molecular plane coincides with the *XY* plane, with the *X* axis being along the direction of maximal extension of the molecule and the *Z* axis perpendicular to the molecular plane. An important aspect of ab initio calculation is the choice of the basis set which describes the electronic distribution reorganization resulting from the external perturbation. It determines both the quality and the cost of the results. Various extended basis sets, including polarization functions and diffuse functions, are generally required for computations of hyperpolarizability. It must be recalled that polarizability is quite sensitive to geometry, and therefore, it is preferable that all geometries be optimized at a common level of theory to avoid geometry effects in the predictions. The calculations have been performed at the MP2 level using the 6-31++G** basis, and all the geometrical parameters of the parent molecules (PNA, *N*-methyl-4-nitroaniline (N-mtPNA), *N*-ethyl-4-nitroaniline (N-etPNA), *N*,*N*-dimethyl-4-nitroaniline (N,N-dmtPNA)) have been optimized at that level of theory using the same basis set. The other geometrical parameters of the molecules in Figure 1 have been

TABLE 1: Dipole Moment (μ), Polarizabilty (α), Hyperpolarizabilities (β and γ), and the HOMO−LUMO Energy Gap (ΔE) of PNA and Its Two Methyl-Substituted Derivatives, PNA-2 and PNA-3[a]

method of property evaluation	HF	HF	MP2	MP2	MP2	MP2
	PNA[b]	PNA[c]	PNA[b]	PNA[c]	PNA-2	PNA-3
μ_X	2.969	3.082	2.697	2.754	2.771	2.63
μ_Y					−0.176	−0.139
μ_Z						
μ	2.969	3.082	2.697	2.754	2.776	2.633
α_{XX}	125.46	131.95	140.36	148.4	156.44	159.71
α_{YY}	92.55	95.82	97.23	101.01	116.89	116.8
α_{ZZ}	48.51	49.17	50.26	50.95	59.31	59.27
α	88.84	92.31	95.95	100.12	110.88	111.92
β_{XXX}	529.06	647.58	837.55	1064.6	1051.4	1007.27
β_{XYY}	−93.28	−106.55	−31.71	−34.1	−28.64	−64.56
β_{XZZ}	−19.98	−21.38	−26.21	−28.47	−27.18	−27.77
β_X	138.60	173.22	259.87	334.01	331.86	304.98
β_{YXX}			−0.16	0.03	−20.96	−4.15
β_{YYY}			0.03	0.06	−5.14	−17.84
β_{YZZ}			−0.1	0.03	−7.64	−15.49
β_Y			−0.08	0.04	−11.25	−12.49
β_{ZXX}			−0.24	−0.02	0.14	−0.88
β_{ZYY}		0.01	0.14	−0.2	0.31	−0.18
β_{ZZZ}			0.02	−0.04	0.05	−0.02
β_Z			−0.03	−0.09	0.17	−0.36
β	138.6	173.22	259.87	334.01	332.05	305.24
γ_{XXXX}	10862	13951	21641	30368	30351	25490
γ_{XXYY}	−242	−375	351	−1480	−203	1341
γ_{ZZXX}	459	449	3893	5108	4072	2886
γ_{YYYY}	1461	713	2406	−4252	4101	6702
γ_{ZZYY}	700	1507	2671	−490	4859	3836
γ_{ZZZZ}	1662	1680	7284	10589	8978	9125
γ	2637	3251	7527	7164	10148	9574
ΔE				0.3717	0.3657	0.3760

[a] The reported values are in atomic units. [b] HF optimized geometry. [c] MP2 optimized geometry.

obtained from the parent molecules by substituting the hydrogen of benzene with a fixed geometry methyl group. The Finite-field perturbation approach is used for the NLO property calculations using the GAMESS-US quantum chemical program. In this work, we have chosen the derivatives based on the energy for the MP2 polarizabilities. An electric field of minimum strength of 0.0010 au is applied for the finite-field calculations of electric field susceptibilities. The orientationally averaged polarizabilities and hyperpolarizabilities given in this paper are obtained from the equations

$$\mu = \sqrt{\mu_x^2 + \mu_y^2 + \mu_z^2} \tag{9}$$

$$\alpha = \frac{1}{3}(\alpha_{XX} + \alpha_{YY} + \alpha_{ZZ}) \tag{10}$$

$$\beta_i = \frac{1}{3}\sum_{k=1}^{3}\beta_{ikk}$$

$$\beta = \sqrt{\beta_X^2 + \beta_Y^2 + \beta_Z^2} \tag{11}$$

$$\gamma = \frac{1}{5}(\gamma_{XXXX} + \gamma_{YYYY} + \gamma_{ZZZZ} + 2\gamma_{XXYY} + 2\gamma_{ZZYY} + 2\gamma_{ZZXX}) \tag{12}$$

The calculated average static first hyperpolarizability, β, can be compared with the experimental quantity, $\beta(-2\omega; \omega, \omega)$, extracted from the solution-phase electric-field-induced second-harmonic generation (EFISH) experiments.[6]

IV. Results and Discussion

The electric field susceptibilities of PNA and its two methyl-substituted derivatives at the ring hydrogen positions are compared in Table 1. Similarly, Tables 2−4 list the axial components of the susceptibility tensors of other parent molecules and their methyl-substituted derivatives as shown in Figure 1. While optimizing geometry, all the atoms except the methyl hydrogens were restricted to the molecular plane. This model planar structure simplifies the computation. A similar strategic approach for the PNA molecule using a [3s2p2d/2s1p] basis set can be found elsewhere.[8] For N-etPNA, a structure with an out-of-plane ethyl group is very low in energy compared with the in-planar N-etPNA. For a comparison, NLO property calculations for the planar N-etPNA and its substituted derivatives with nonplanar geometry were also carried out. The results are given in Table 5.

In these model calculations, our attention has been restricted mainly to linear response coefficients, α_{ij}, and the main tensor elements of the nonlinear response coefficients which are arising because of the polarization in the molecular plane. Table 1 reports the nonlinear optical coefficients of PNA for two different geometries, the SCF optimized geometry and the MP2 optimized geometry. At this point, it is worthwhile to remark on the comparison between the calculations performed for PNA molecule using MP2 optimized geometry and HF optimized geometry. For the same level of property evaluation, the MP2

TABLE 2: Calculated Dipole Moment (μ), Polarizabilty (α), and Hyperpolarizabilities (β and γ) and the HOMO−LUMO Energy Gap (ΔE) of N-mtPNA Compared with the Values of Its Four Methyl-Substituted Derivatives, N-mtPNA-2, N-mtPNA-3, N-mtPNA-5, and N-mtPNA-6[a]

	N-mtPNA	N-mtPNA-2	N-mtPNA-3	N-mtPNA-5	N-mtPNA-6
μ_X	2.95	3.097	2.842	2.807	2.941
μ_Y	0.272	0.167	0.127	0.391	0.454
μ_Z					
μ	2.963	3.101	2.845	2.834	2.976
α_{XX}	172.77	179.84	183.82	184.69	179.64
α_{YY}	110.93	125.45	126.71	126.31	128.07
α_{ZZ}	60.06	66.8	68.26	68.29	68.24
α	114.59	124.03	126.27	126.43	125.32
β_{XXX}	1343.22	1267.46	1265.4	1270.26	1317.38
β_{XYY}	−44.18	−30.41	−77.33	−69.92	−38.76
β_{XZZ}	−21.16	−6.82	−21.08	−0.41	−16.33
β_X	425.96	410.08	389.00	399.97	420.76
β_{YXX}	67.32	51.31	72.05	69.15	94.93
β_{YYY}	−3.15	−9.69	−24.94	10.09	2.87
β_{YZZ}	13.79	−5.08	−0.59	28.82	23.69
β_Y	25.99	12.18	15.51	36.02	40.50
β_{ZXX}	0.98	1.66	1.55	−16.69	0.89
β_{ZYY}	0.44	1.76	0.6	0.27	1.69
β_{ZZZ}	1.52	1.84	0.67	0.44	1.78
β_Z	0.98	1.76	0.94	−5.32	1.45
β	426.76	410.26	389.31	401.63	422.71
γ_{XXXX}	41191	43162	35206	34588	41284
γ_{XXYY}	1995	3635	1489	4385	7320
γ_{ZZXX}	4917	5434	7016	5242	838
γ_{YYYY}	6959	7083	6321	7275	5257
γ_{ZZYY}	6607	6810	6769	6505	7752
γ_{ZZZZ}	13676	10129	13153	10380	13727
γ	17773	18426	17046	16902	18417
ΔE	0.3652	0.3585	0.3711	0.3684	0.3598

[a] The listed values are in atomic units.

optimized geometry gives a higher dipole moment value and higher linear and nonlinear optical coefficients. When comparing the property evaluation at the MP2 level for both the SCF (column 3) and MP2 geometries (column 4), we observe that, although the hyperpolarizabilities along the molecular axis follow the trend observed for the polarizabilities along the same axis, the average value of γ is less for an MP2 geometry than that of an SCF geometry. Since both the geometries are very similar, there are no dramatic changes in the coefficients obtained from the same level of theory. However, this conclusion might not be valid for systems in which the HF−SCF method yields a poor geometry. It is interesting to note that, for a fixed geometry, SCF and MP2 yield entirely different susceptibility values. The percentage of change becomes larger and larger as the order of susceptibility increases. For example, in the case of an MP2 optimized geometry, the γ obtained by MP2 calculation is twice that of the γ obtained by HF calculation. The same is true for the β value also, and the percentage of increment is around 80. Except for a couple of terms, the MP2 values for the dipole moment, the axial components of polarizability, and the tensor components of hyperpolarizability are quite clearly higher than those of corresponding SCF results. This is not surprising, since the higher-order susceptibilities demand more electron correlation, as the contribution of higher-energy states in these susceptibilities is higher. Thus, the predictions based on the Hartree−Fock level are not very rigorous. To obtain reasonable values for the various individual contributions to the hyperpolarizability, it is necessary to include electron correlation. Qualitative results for the relative importance of these contributions can often be obtained at the HF level, but beyond that, correlation must be included for this purpose as well. A comparison for a PNA molecule between MP2 and HF−SCF property evaluation from Table 1 indicates that the MP2 method adequately reproduces the effect of correlation on the relative magnitude of the various contributions to each property and gives a reasonable prediction for the individual values. Our observations about the PNA also agree with the other theoretical calculations available in the literature.[6,8]

TABLE 3: Calculated Dipole Moment (μ), Polarizabilty (α) Hyperpolarizabilities (β and γ), and the HOMO−LUMO Energy Gap (ΔE) of N,N-dmtPNA and Its Two Methyl-Substituted Derivatives, N,N-dmtPNA-2 and N,N-dmtPNA-3

	N,N-dmtPNA	N,N-dmtPNA-2	N,N-dmtPNA-3
μ_X	3.1	3.258	2.971
μ_Y	−0.004	−0.1	−0.13
μ_Z			
μ	3.1	3.259	2.974
α_{XX}	193.2	198.89	204.75
α_{YY}	123.57	75.89	138.95
α_{ZZ}	69.43	138.86	77.51
α	128.73	137.88	140.4
β_{XXX}	1587.41	1471.63	1496.38
β_{XYY}	−72.82	−56.86	−98.73
β_{XZZ}	−28.41	−19.15	−24.65
β_X	495.40	465.21	457.67
β_{YXX}	−3.5	−17.04	−0.24
β_{YYY}	−0.02	−21.07	−16.6
β_{YZZ}	0.59	−27.09	−13.67
β_Y	−0.97	−21.73	−10.17
β_{ZXX}	0.46	0.95	0.9
β_{ZYY}	0.03	0.94	0.92
β_{ZZZ}	−0.14	0.79	0.49
β_Z	0.12	0.89	0.77
β	495.4	465.72	457.78
γ_{XXXX}	47895	51223	37287
γ_{XXYY}	1523	3078	−1975
γ_{ZZXX}	5807	6642	3695
γ_{YYYY}	6822	5367	2029
γ_{ZZYY}	2190	7314	4371
γ_{ZZZZ}	12056	13510	9577
γ	17162	20834	12215
ΔE	0.3598	0.3534	0.3644

From a chemical perspective, the most important feature of the NLO response calculation is the insight that they provide into the effect of subtle variations in the molecular architecture on the NLO responses. While analyzing the relationship between the chemical structure and the second-order nonlinear properties, we observe that second-order NLO effects in organic molecules originate from a strong donor−acceptor intramolecular interaction. Davydov et al.[10] showed that dipolar aromatic molecules possessing an electron donor group and an acceptor group contribute to large second-order optical nonlinearity arising from the intramolecular charge transfer between two groups of opposite nature. Therefore, a typical SHG-active molecule can be presented as a donor−π-conjugate-bridge−acceptor system, if it lacks a center of symmetry. On the other hand, a π-conjugate molecule with a donor and an acceptor will not display SHG activity if it possesses a center of symmetry. Hence, while designing the NLO material, more attention has been focused on the donor−acceptor tailoring, symmetry, and geometry requirements.[12] Much interest in second-order NLO properties of substituted benzene derivative systems stems from the basic studies of the chemistry and physics of PNA. Here, variation in NLO response with tailored architecture in PNA is studied from PNA derivatives obtained by substituting the hydrogen in the NH_2 group and the benzene ring with a methyl group. In a

TABLE 4: Calculated Dipole Moment (μ), Polarizabilty (α), and Hyperpolarizabilities (β and γ) and the HOMO−LUMO Energy Gap (ΔE) of N-etPNA and Its Methyl-Substituted Derivatives[a]

	N-etPNA	N-etPNA-2	N-etPNA-3	N-etPNA-5	N-etPNA-6
μ_X	3.108	3.196	3.015	2.956	3.069
μ_Y	0.481	0.355	0.333	0.585	0.677
μ_Z	0.013	0.011	0.012	0.012	0.012
μ	3.145	3.216	3.033	3.013	3.142
α_{XX}	193.99	209.34	204.61	206.77	200.35
α_{YY}	121.47	133.29	137.34	136.13	138.98
α_{ZZ}	68.45	73.4	76.47	76.64	76.39
α	127.97	138.68	139.48	139.85	138.57
β_{XXX}	1533.96	1420.46	1425.98	1446.22	1494.49
β_{XYY}	−19.54	13.22	−27.31	−37.38	275.76
β_{XZZ}	−3.83	−11.06	−10.53	−13.94	−5.45
β_X	503.53	474.21	462.71	464.97	588.27
β_{YXX}	−2.77	220.58	246.84	231.64	6.78
β_{YYY}	247.49	−29.27	−49.45	−18.48	−14.96
β_{YZZ}	−6.19	−17.55	−16.31	10.46	−0.98
β_Y	79.51	57.92	60.36	74.54	−3.05
β_{ZXX}	−11.56	−2.64	−3.9	−1.6	−9.64
β_{ZYY}	1.4	3.2	4.26	4.15	8.14
β_{ZZZ}	0.2	1.36	0.55	0.15	−4.54
β_Z	−3.32	0.64	0.30	0.90	−2.01
β	509.78	477.73	466.63	470.9	588.28
γ_{XXXX}	47657	48274	40116	40494	52887
γ_{XXYY}	4274	5112	2380	3089	5275
γ_{ZZXX}	4362	5083	3760	2609	4484
γ_{YYYY}	6403	10729	7927	5271	9210
γ_{ZZYY}	4142	6151	5053	3243	5715
γ_{ZZZZ}	7226	7783	6853	4448	7728
γ	17369	19896	15456	13619	20155
ΔE	0.3611	0.3563	0.3619	0.3605	0.3555

[a] The reported values are in atomic units.

TABLE 5: Calculated Dipole Moment (μ), Polarizabilty (α), and Hyperpolarizabilities (β and γ) and the HOMO−LUMO Energy Gap (ΔE) of N-etPNA and Its Methyl-Substituted Derivatives[a]

	N-etPNA	N-etPNA-2	N-etPNA-3	N-etPNA-5	N-etPNA-6
μ_X	2.387	2.499	2.387	2.387	2.387
μ_Y	0.505	0.349	0.344	0.63	0.678
μ_Z	−0.055	−0.081	−0.036	−0.035	−0.076
μ	2.44	2.525	2.412	2.469	2.482
α_{XX}	176.01	191.81	176.01	176.01	176.01
α_{YY}	121.32	133.48	137.31	136.68	137.43
α_{ZZ}	73.6	80.59	81.7	81.85	81.67
α	123.65	135.29	131.67	131.52	131.71
β_{XXX}	912.44	872.25	912.44	912.44	912.44
β_{XYY}	−21.16	3.79	−39.31	−43.63	−8.62
β_{XZZ}	−21.9	−18.83	−19.17	−26.11	−24.91
β_X	289.79	285.74	284.65	280.90	292.97
β_{YXX}	123.06	97.04	113.45	126.32	133.17
β_{YYY}	−2.83	−15.79	−36.59	5.85	16.68
β_{YZZ}	5.27	−6.98	−8.07	15.73	17.27
β_Y	41.84	24.76	22.93	49.30	55.70
β_{ZXX}	−169.82	−162.12	−166.13	−166.9	−164.15
β_{ZYY}	−5.19	3.79	0.05	−0.75	−4.74
β_{ZZZ}	−10.15	−7.54	−10.33	−9.75	−1.72
β_Z	−61.72	−55.29	−58.80	−59.13	−56.87
β	299.23	292.09	291.56	291.26	303.59
γ_{XXXX}	33509	35650	33509	33509	33509
γ_{XXYY}	2972	5064	4036	5666	4695
γ_{ZZXX}	3035	4259	4928	4741	5930
γ_{YYYY}	5309	5472	5669	8345	8033
γ_{ZZYY}	2369	2464	3067	3882	3367
γ_{ZZZZ}	5000	6558	6502	6529	6869
γ	12114	14251	13948	15392	15279
ΔE	0.3740	0.3657	0.3778	0.3775	0.3687

[a] The reported values are in atomic units. The parent molecule (N-etPNA) is nonplanar in geometry, and the derivatives are obtained by substituting the ring −H atom of this nonplanar molecule with $-CH_3$ group.

covalent single bond between unlike molecular fragments, the electron pair forming a σ bond is never shared absolutely equally between the two fragments: it tends to be attracted more toward the electron-deficient fragment of the two. This influence of electron distribution in the σ bond is known as the inductive effect,[29] and the methyl group attached to C or N of the PNA molecule exerts such an electron-donating inductive effect in the direction of the other fragment. Though the effect is quantitatively rather small, it is responsible for the increase in basicity that results when one of the H atom of ammonia is replaced by a CH_3 group and, in part at any rate, for the readier substitution of the aromatic nucleus in methyl benzene than in benzene itself. All inductive effects are permanent polarizations in the ground state of a molecule and are therefore manifested in its physical properties, for example, its dipole moment.

The substitution of a methyl group at the second C carbon of the benzene ring (PNA-2) does not change the dipole moment and the average value of β much compared to the parent PNA molecule, whereas the substitution of a methyl group at third C (PNA-3) decreases both values (all the values are given in Table 1). In both the substitutions, the average values of α and γ are larger than that of the parent molecule, and the γ increment is about 90% of that of PNA. Although the *Y* components of the β vector for PNA-3 is larger in magnitude, the β_{XXX} value is less in magnitude compared with the PNA-2 and PNA molecules. The molecular orbital picture can be used to predict the trend in β with varying substitution patterns. Because of charge transfer, the absorption band of an organic dye with a π-conjugated donor−acceptor system can be tailored by either increasing the π-conjugation length or by substituting donor−acceptor groups to a conjugated system. As a result, the absorption band of the UV−vis spectrum can be shifted and will have either bathochromic or hypsochromic features. Electron donor−acceptor groups cause bathochromic shifts which also increase the intensity of the absorption bands.[30] A donor group can increase the electron density in the π-conjugated system, leading to a strong interaction from the donor−acceptor combination. The donor−acceptor interaction is also affected by the relative position of the π-conjugated system. This changes the charge transfer and the electronic distribution.

PNA, which is the basic molecule for organic NLO, consists of a benzene ring in which an electron donor amino (NH_2) group is substituted in a para position to an electron acceptor nitro (NO_2) group. These opposite ends of the conjugated system lead to maximum acentricity in the molecule. The π electron donor and acceptor configuration composed of NH_2 and NO_2, respectively, in PNA results in intramolecular charge transfer interactions. The PNA molecule exhibits extremely large first hyperpolarizability (β) due to the highly asymmetric charge distribution arising from the π electronic structure of the molecule. Moreover, in the PNA molecule, intramolecular charge transfer interaction is prominent because of a desirable resonance structure leading to large β. Its highly asymmetric charge-correlated excited states of the π electron structure also contribute to the large β value. But in practice, the PNA molecule crystallizes in a centrosymmetric space group, which restricts the observation of any macroscopic second-order optical effect. Therefore, closely related PNA derivatives, which do not have centers of symmetry in the crystalline state, have been considered here. When the benzene ring of PNA is substituted with a CH_3 group, the resulting chemical substitution provides

TABLE 6: Calculated Dipole Moment (μ), Polarizability (α), Hyperpolarizabilities (β and γ), and the HOMO−LUMO Energy Gap (ΔE) of PNA Compared with the Values for N-mtPNA, N,N-dmtPNA, and N,N-dmtPNA[a]

	PNA	N-mtPNA	N,N-dmtPNA	N-etPNA
μ_X	2.754	2.95	3.1	3.108
μ_Y		0.272	−0.004	0.481
μ_Z				0.013
μ	2.754	2.963	3.1	3.145
α_{XX}	148.4	172.77	193.2	193.99
α_{YY}	101.01	110.93	123.57	121.47
α_{ZZ}	50.95	60.06	69.43	68.45
α	100.12	114.59	128.73	127.97
β_{XXX}	1064.6	1343.22	1587.41	1533.96
β_{XYY}	−34.1	−44.18	−72.82	−19.54
β_{XZZ}	−28.47	−21.16	−28.41	−3.83
β_X	334.01	425.96	495.40	503.53
β_{YXX}	0.03	67.32	−3.5	−2.77
β_{YYY}	0.06	−3.15	−0.02	247.49
β_{YZZ}	0.03	13.79	0.59	−6.19
β_Y	0.04	25.99	−0.97	79.51
β_{ZXX}	−0.02	0.98	0.46	−11.56
β_{ZYY}	−0.2	0.44	0.03	1.4
β_{ZZZ}	−0.04	1.52	−0.14	0.2
β_Z	−0.09	0.98	0.12	−3.32
β	334.01	426.76	495.4	509.78
γ_{XXXX}	30368	41191	47895	47657
γ_{XXYY}	−1480	1995	1523	4274
γ_{ZZXX}	5108	4917	5807	4362
γ_{YYYY}	−4252	6959	6822	6403
γ_{ZZYY}	−490	6607	2190	4142
γ_{ZZZZ}	10589	13676	12056	7226
γ	7164	17773	17162	17369
ΔE	0.3717	0.3652	0.3598	0.3611

[a]The reported values are in atomic units.

TABLE 7: Comparison of Dipole Moment (μ), Polarizability (α), Hyperpolarizabilities (β and γ), and the HOMO−LUMO Energy Gap (ΔE) of Symmetric Molecules (PNA-2,6 and PNA-3,5) with Asymmetric Molecules (PNA-2 and PNA-3)[a]

	PNA-2	PNA-2,6	PNA-3	PNA-3,5
μ_X	2.771	2.785	2.63	2.496
μ_Y	−0.176	0.000	−0.139	0.000
μ_Z		0.000		0.000
μ	2.776	2.785	2.633	2.496
α_{XX}	156.44	164.26	159.71	169.90
α_{YY}	116.89	133.41	116.8	133.14
α_{ZZ}	59.31	67.55	59.27	67.44
α	110.88	121.74	111.92	123.49
β_{XXX}	1051.4	1038.91	1007.27	940.80
β_{XYY}	−28.64	−17.23	−64.56	−94.80
β_{XZZ}	−27.18	−27.19	−27.77	−29.44
β_X	331.86	331.50	304.98	272.19
β_{YXX}	−20.96	0.12	−4.15	0.51
β_{YYY}	−5.14	0.10	−17.84	−0.02
β_{YZZ}	−7.64	0.21	−15.49	0.11
β_Y	−11.25	0.14	−12.49	0.20
β_{ZXX}	0.14	−0.01	−0.88	−0.19
β_{ZYY}	0.31	0.15	−0.18	−0.32
β_{ZZZ}	0.05	0.12	−0.02	0.05
β_Z	0.17	0.09	−0.36	−0.15
β	332.05	331.50	305.24	272.19
γ_{XXXX}	30351	29916	25490	22247
γ_{XXYY}	−203	1325	1341	1199
γ_{ZZXX}	4072	4356	2886	1016
γ_{YYYY}	4101	5418	3836	3616
γ_{ZZYY}	4859	6391	6702	3591
γ_{ZZZZ}	8978	10071	9125	4146
γ	10148	13910	12061	8325
ΔE	0.3657	0.3621	0.3760	0.3749

[a]The reported values are in atomic units.

the maximum acentricity to the molecule and gives rise to a non-centrosymmetric crystal structure. In PNA-2 and PNA-3, the asymmetric derivatives of PNA, the first one gives the higher β, which can be explained as follows. Since a major contribution to β is due to charge transfer, one will get higher β with the factors which enhance the charge transfer. The highest occupied molecular orbital (HOMO)−lowest unoccupied (LU)MO gap (optical gap) in the molecular orbital picture plays a vital role in the charge transfer.[12] If the gap is small, it is very easy for the charge transfer to occur. Thus, the HOMO largely dictates the source of charge transfer, and the details of the molecular LUMO govern the acceptor portion of the excitation. One can tailor the asymmetry of the electron density by tuning the energetic HF−SCF of the appended substituents. The HOMO−LUMO gaps (ΔE) of the molecules are given in Tables 1−7. In the case of methyl substitution at the second carbon, one more donor group is added near to the parent donor group, while in the substitution at the third carbon, the added donor group is nearer to the acceptor group. This provides a higher HOMO energy and a lower LUMO energy for PNA-2 than that of PNA-3. This leads to a smaller HOMO−LUMO energy gap for the former, and clearly, the former one has a greater β value than the latter. This shows that substitution of H with a methyl group (electron-donating group) at the second C of the benzene ring increases the HOMO energy. The electron density of the HOMO orbital, which is confined more to the electron-donating group ($-NH_2$), will favor the charge transfer to the LUMO orbital, confined toward the electron acceptor part ($-NO_2$) of the molecule. On the other hand, substituting at the third C with a methyl group increases the LUMO energy, and a higher LUMO would not favor a charge transfer from a HOMO. Furthermore, on the basis of the orientation of the ring substitution by different groups, substitution in position 2 is more favorable. Position 2 is ortho to the NH_2 group (ortho and para directing) and meta to the NO_2 group (meta directing) of PNA.

From the two-level model, using electric dipole moment approximation, the second harmonic generation response (SHG) can be written as[31]

$$\beta_{\text{two-level}} = \frac{3e^2}{2\hbar} \frac{\omega_{12} f \Delta\mu}{(\omega_{12}^2 - \omega^2)(\omega_{12}^2 - 4\omega^2)} \qquad (13)$$

Where $\hbar\omega_{12}$ is the excitation energy, f the oscillator strength, $\Delta\mu$ the difference between the dipole moments of the ground and the excited state, and the ω specifies the excitation frequency of the oscillating electric field. The most important factor in the above expression is that the SHG coefficient is directly proportional to the oscillator strength, f, and the dipole moment difference, $\Delta\mu$, and is inversely proportional to the optical gap. Thus, any phenomenon that decreases the gap and increases the dipole moment difference between the ground and excited states will enhance β. So, it is very clear from Table 1 that methyl substitution at the second carbon will lead to a higher β value. The α and γ values can also be greatly boosted by the donor−acceptor push−pull phenylenes in which the donor−acceptor-substituted benzene shows larger optical nonlinearity than the unsubstituted ones.[30]

N,N-dmtPNA also has the same symmetry point group as PNA. N,N-dmtPNA and its two derivatives (Table 3) also show a similar trend observed in Table 1 for the average value of the susceptibilities except for the γ values. The molecular orbital

picture is also similar. The γ value of the N,N-dmtPNA-2 molecule is 20% higher than that of the parent molecule. The γ value for N,N-dmtPNA-3 is lower than that of the parent molecule. In both the PNA and N,N-dmtPNA parent molecules, the 2-substituted derivative has a higher β value than that of the 3-substituted derivative, whereas the average value of α is higher for a 3-substituted derivative.

For an unsymmetrical N-mtPNA (Table 2) and N-etPNA (Table 4), the 2- and 6-substituted derivatives show higher α values than the parent and other substituted molecules. In these cases, the 2- and 6-substituted derivatives have larger γ values than the parent and other substituted derivatives. The β values for 2- and 6-substituted derivatives are larger than those of 3- and 5-substituted derivatives. For N-etPNA, the 6-substituted derivatives have larger β and γ values than the 2-substituted derivative. The observed trend in β can be interpreted in terms of SCF energy. The substitution of H with a methyl group at the second and sixth positions increases the HOMO energy, and the substitution at the third and fifth positions increases the LUMO energy. The HOMO−LUMO energy gap is at a minimum for the molecules derived from the substitutions at the second and sixth positions of the benzene ring. Here also, positions 2 and 6 are nearer to the parent donor molecule, thus giving an additive effect to the donor contribution compared to 3 and 5. Positions 2 and 6 are orientationally more favorable for substitution, since both are ortho to the NH_2 and meta to the NO_2 of PNA. It should be noted that the β value of N-etPNA-6 is larger compared to those of N-etPNA-2 and N-etPNA. There can be two possible reasons for this observation. The first is the magnitude of the optical gap as mentioned earlier. The second is the steric effect, created by the crowding of the spatially adjacent amino $-C_2H_5$ group and $-CH_3$ at the second C position of the benzene ring. This means that the p orbitals on nitrogen and the ring carbon atom, to which it is attached, are prevented from becoming parallel to each other, and their overlap is thus inhibited. Electronic interaction with the nucleus is largely prevented, and the transfer of charge does not take place from amino group to nitro group. Since we have fixed our geometry to a planar one, the reason for the lower β value would be coming from the nonplanar excited-state geometry of N-etPNA-2. This nonplanar excited-state assistance in the β value would not be affecting the N-etPNA-6 molecule, as the molecule is free from steric effects. The relative lowering of the β values of N-mtPNA-2 and N,N-dmtPNA-2 as compared to those of PNA-2 can also be explained on the basis of the above-mentioned steric effect. The PNA-2 molecule is free from steric effects, as there is no $-CH_3$ group in the amino nitrogen.

The experiment-related quantities such as Hyper Rayleigh scattering (HRS) β and the associated depolarization ratios can be used for the study of the structure−property relationship and symmetric effect. These orientationally averaged quantities have been calculated by Bersohn et al. for linearly polarized incident radiation for several high-symmetry point groups.[32] The expressions for these orientationally averaged quantities can be found elsewhere.[32,33] The orientationally averaged depolarization ratios for PNA and its substituted derivatives have been calculated. However, the variation of the depolarization ratio as a function of substituent in the present case is not very useful to study the structural−property relations, and the symmetric effects as the depolarization ratios calculated in all the cases are $\cong$0.2. The experimental value of the incoherent depolarization ratio using HRS studies for PNA in methanol and chloroform was estimated to be 0.23.[34] The electric field response coefficients of PNA and its higher-order methyl derivatives obtained by replacing amino hydrogens are given in Table 6. As we go from PNA to higher-order derivatives, all the NLO coefficients become larger with respect to the number of methyl groups added. The γ value of N-mtPNA is larger than that of its higher-order methyl derivatives. The HOMO−LUMO gap becomes smaller as the number of methyl groups increases in the amino nitrogen. The nitrogen becomes more electron-rich and favors a high charge transfer to the LUMO. It is interesting to note that the β values of the isoelectronic N,N-dmtPNA and N-etPNA do not agree with the additive rule of methyl addition. Although the latter one possesses a high HOMO−LUMO gap, it has a higher β value. This observation can be interpreted using the well-known symmetric effect in nonlinear optics. In line with Neumann's principle, which states that the physical properties of a system are invariant to its symmetry operations, the susceptibility tensors have the symmetry properties of the medium and thus can restrict the combinations of vector components of the various optical fields that could practically be used. For instance, the odd susceptibility terms are always nonzero, while the even terms can be vanishing because of the center of symmetry. Thus, to have effects driven by second-order nonlinear susceptibility terms, it is important to have a non-centrosymmetric medium. The even order nonlinear coefficient becomes prominent only if the molecule is less symmetric. Clearly, N-etPNA is asymmetric, while N,N-dmtPNA possesses C_{2v} symmetry. The β value does not grow additively as we move from PNA to its higher-order derivatives. This is true because N-mtPNA is asymmetric, while PNA and N,N-dmtPNA are symmetric in nature. To put this issue of symmetry factor in further perspective, we focus on the study of the molecules derived by substituting two hydrogen atoms of the benzyl ring of PNA with two methyl groups. The HOMO−LUMO gap of PNA-2 is higher than that of its higher methyl derivative, PNA-2,6. But the PNA-2,6 has a smaller β value than PNA-2, irrespective of the addition of one more electron-pushing methyl group at the sixth position of PNA-2. This smaller β value for PNA-2,6 is due to the fact that a nonsymmetric PNA-2 becomes C_{2v}-symmetric when a CH_3 group is added to the sixth position of PNA-2. The same is true for a PNA-3 and PNA-3,5 pair. While studying the geometrical effect on the NLO coefficients, we compared planar and nonplanar N-etPNA and its derivatives. It is observed that the coefficients β and γ are very large in planar system compared to nonplanar ones; α also increases slightly because of planarity. From the very classical insight about charge transfer, it is very clear that, for a continuous charge transfer to occur, systems should be planar. Since β and γ depend more on charge transfer compared to α, those coefficients are much larger in planar geometries. It can be also observed that the systems with substitution at nitrogen (NH_2 group) give higher values for all the coefficients than the isoelectronic counterparts with ring substitution. By comparing the dipole moment and the optical gap of these systems, it can be explained that the substitution at nitrogen increases the donor strength, hence favoring the charge transfer, even though the dipole moment is almost the same for most of the pairs.

V. Conclusion

Since charge transfer plays an important role in NLO processes, the systems having more favorable features for charge transfer give higher nonlinear coefficients. Hence, strength and number of donors and acceptors, asymmetry, and geometry of the systems and positions of the substitutions play important roles in determining NLO response. Out of the possible structures, many can readily be described on the basis of simple

considerations (the sigmatropic effect of the methyl substitutions on NH_2 group, position of substitution in the benzene ring, etc.), but more quantitative assessments require direct quantum mechanical calculations of the electric field response. Factors such as structure, primary and secondary, and the resulting electron density distribution turn out to have a great influence on these properties. High electric susceptibilities depend on the nature of the delocalized structures, and it is the purpose of molecular design in optoelectronics to find molecular systems that yield the largest possible responses. The larger these linear and nonlinear responses are, the smaller the electric field required to achieve the desired electrooptic effect. As already pointed out, the molecular structure of organic materials can be modified in order to maximize the electric responses.

Acknowledgment. Y. S. acknowledges Council of Scientific and Industrial Research (CSIR), New Delhi, for financial support.

References and Notes

(1) Chemla, D. S.; Zyss, J. *Nonlinear Optical Properties of Organic molecules and Crystals*; Academic Press: New York, 1987; Vol. 1

(2) Finn, R. S.; Ward, J. F. *Phys. Rev. Lett.* **1971** *26*, 285; *J. Chem. Phys*. **1974**, *60*, 454. Ward, J. F.; New, G. H. C. *Phys. Rev.* **1969**, *185*, 57.

(3) Buckingham, A. D.; Orr, B. J. *Trans. Faraday Soc*. **1969**, *65*, 673. Brown, J. M.; Buckingham, A. D.; Ramsey, D. A. *Can. J. Phys.* **1969**, *49*, 914.

(4) Bartlett, R. J.; Purvis, G. D. *Phys. Rev. A* **1979**, *20*, 1313.

(5) Butcher, P. N.; Cotter, D. *The Elements of Nonlinear Optics*; Night, P. L., Firth, W. J., Eds.; Cambridge University Press: Cambridge, England, 1990.

(6) Daniel, C.; Dupuis, M. *Chem. Phys. Lett.* **1990**, *171*, 209.

(7) Perrin, E.; Prasad, P. N.; Mougenot, P.; Dpuis, M. *J. Chem. Phys.* **1989**, *91*, 4728.

(8) Sim, F.; Chin, S.; Dupuis, M.; Rice, J. E. *J. Phys. Chem.* **1993**, *97*, 1158.

(9) Sekino, H.; Bartlett, R. J. *J. Chem. Phys.* **1986**, *85*, 976. Liu, S. Y.; Dykstra, C. E. *J. Phys. Chem.* **1987**, *71*, 1749.

(10) Davydov, B. L.; Derkacheva, L. D.; Dunina, V. V.; Zhabotinski, M. K.; Zolin, V. K.; Kreneva, L. G.; Samokhina, M. A. *JETP Lett*. **1970**, *12*, 16.

(11) Moylan, C. R. *J. Phys. Chem*. **1994**, *98*, 13513.

(12) Kanis, D. R.; Ratner, M. A.; Marks, T. J. *Chem. Rev.* **1994**, *94*, 195.

(13) Albert, I. D. L.; Morley, J. O.; Pugh, D. *J. Chem. Phys*. **1995**, *102*, 237.

(14) Champagne, B.; Kirtman, B. *Handbook of Advanced Electronic and Photonic Materials*; Nalwa, H. S., Ed.; Academic: San Diego, 2001; Vol. 9, Chapter 2, p 63.

(15) Morley, J. *J. Chem. Soc., Perkin Trans.* **1995**, *2*, 177; **1994**, 2, 1211; *J. Phys Chem.* **1994**, *98*, 11818.

(16) Bishop, D. M. *Adv. Chem. Phys.* **1998**, *104*, 1.

(17) Ågren, H.; Vahtras, O.; Koch, H.; Jørgensen, P.; Helgaker, T. *J. Chem. Phys*. **1993**, *98*, 6417.

(18) Mikkelsen, K. V.; Luo, Y.; Ågren, H.; Jørgensen, P. *J. Chem. Phys*. **1994**, *102*, 9362.

(19) Champagne, B.; Perpete, E. A.; Jacquemin, D.; van Gisbergen, S. J. A.; Baerends, E.-J.; Soubra-Ghaoui, C.; Robins, K. A.; Kirtman, B. *J. Phys. Chem. A* **2000**, *104*, 4755.

(20) Champagne, B. *Chem. Phys. Lett.* **1996**, 261. 57.

(21) Quineta, O.; Champagne, B.; Kirtmanb, B. *THEOCHEM* **2003**, *633*, 199.

(22) Orr, B. J.; Ward, J. F. *Mol. Phys*. **1971**, *20*, 513.

(23) Li, D.; Ratner, M. A.; Marks, T. J. *J. Am. Chem. Soc*. **1988**, *110*, 1707.

(24) Cohen, H. D.; Roothan, C. C. J. *J. Chem. Phys.* **1965**, *43*, S34.

(25) Waite, J.; Papadopoulos, M. G. *J. Phys. Chem*. **1989**, *93*, 43.

(26) Sekino, H.; Bartlett, R. J. *J. Chem. Phys.* **1986**, *85*, 976. Karna, S. P.; Dupuis, M. *J. Comput. Chem.* **1991**, *12*, 487.

(27) Hättig, C.; Hess, B. A. *Chem. Phys. Lett.* **1995**, *233*, 359.

(28) Rozyczko, P. B.; Perera, A. S.; Nooijen, M.; Bartlett, R. J. *J. Chem. Phys*. **1997**, *107*, 6736.

(29) Sykes, P. *A guide book to mechanism in inorganic chemistry*; Orient Longman: New Delhi, 1986.

(30) Nalwa, H. S.; Miyata, S. *Nonlinear Optics of Organic Molecules and Polymers*; CRC Press: New York, 1997.

(31) Oudar, J. L.; Chemla, D. S. J. *Chem. Phys*. **1977**, *66*, 2664. Oudar, J. L. *Chem. Phys*. **1977**, *67*, 446.

(32) Bersohn, R.; Pao, Y. H.; Frisch, H. L. *J. Chem. Phys.* **1966**, *45*, 3184.

(33) Heesink, G. J. H.; Ruiter, A. G.; van Hulst, N. F.; Bolger, B. *Phys. Rev. Lett*. **1993**, *71*, 999.

(34) Janssen, R. H. C.; Theodourou, D. N.; Raptis, S.; Papadopoulos. M. G. *J. Chem. Phys.* **1999**, *111*, 9711.